Article

Battling Retardation and Nonlocality: The Hunt for the Ultimate Plasmonic Cascade Nanolens
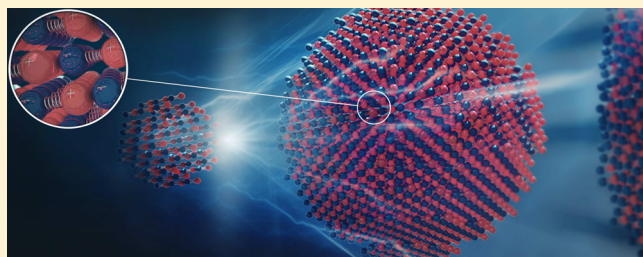
Jamie M. Fitzgerald*,[†] and Vincenzo Giannini[†,‡]

[†]Department of Physics, Condensed Matter Theory, Imperial College London, London SW7 2AZ, United Kingdom

[‡]Instituto de Estructura de la Materia (IEM-CSIC), Consejo Superior de Investigaciones Científicas, Serrano 121, 28006 Madrid, Spain

ABSTRACT: The plasmonic nanolens was proposed as a deterministic method to achieve high field enhancements and, hence, enable single molecule photonic devices, but experimental results have failed to live up to these expectations, and recent theoretical works have brought its long-assumed advantages into doubt. To explore the limits of cascade field enhancements, we consider possible quantum solutions ("going small") and use phononic materials at longer wavelengths ("going large"). We find that entering the quantum plasmonic limit to enhance the size ratio between constituent nanoparticles is not a fruitful strategy, as the increased electron-surface scattering decreases the field enhancement by over an order of magnitude. Using larger nanoparticles is limited in metals by retardation, but using localized surface phonon polaritons, which can be excited in polar dielectrics, is an effective strategy due to the lower energy phonon frequency and high quality factor. We compare the nanolens against the more usual dimer configuration and find that the superior geometry depends crucially on the material used, with noble metal nanolenses unlikely to offer better performance to equivalent dimers. In contrast, SiC nanolenses can offer a larger maximum field enhancement, up to 10^4, compared to the corresponding dimer configuration, suggesting that future endeavors in constructing nanolenses should be based on polar dielectrics. This could have wide-ranging implications for IR/THz surface-assisted spectroscopies.

KEYWORDS: *localized plasmons, plasmonic nanolens, plasmonic dimer, silicon carbide, field enhancement, nonlocality*

Research in plasmonics has ushered in a new era of precise control over light in subdiffraction volumes.[1] One of the most famous examples of this is the nanolens, first proposed by Li et al. in 2003,[2] where a finite chain of self-similar metallic nanospheres, which support localized surface plasmons (LSPs), are used to concentrate light to a "hot spot" via a cascade effect. Enhancements on the order of 10^3 were predicted, which is desirable for applications in sensing,[3] energy conversion,[4] nonlinear plasmonics,[5] and surface-enhanced Raman spectroscopy (SERS)[6] (with potential for single molecule detection), among others. Despite the complex structure, there has been a number of experimental realizations[7−15] and continuing efforts. For instance, silver nanolenses self-assembled by DNA origami scaffolds have been recently demonstrated.[16]

The original proposition[2] for the nanolens was formulated within the quasistatic regime, which limits the size of the constituent nanoparticles to below a few tens of nms for plasmonics in the visible. In subsequent work,[17,18] full electrodynamic simulations have shown that retardation effects limit the achievable field enhancement (FE) considerably. Thus, it seems sensible to stay within the electrostatic regime when designing a nanolens, but a large size difference between the nanoparticles is essential for a strong nanolensing effect. Unfortunately, this is experimentally difficult to realize. Further, for nanoparticles less than about 10 nm in size, nonlocal effects

start to become important[19−24] and will shift the LSP resonance and decrease the maximum FE achievable. Nonlocality in small nanoparticles is a consequence of the finite extent of the electronic wave functions which results in a smeared-out screening charge at metallic interfaces, rather than the infinitesimally thin layer assumed by classical electromagnetism. To describe this within the framework of classical electromagnetic methods, a spatially dispersive longitudinal dielectric function is necessary. Nonlocal effects are also important for small gaps where it leads to effective increase in the separation of the particles,[23,25] also reducing the FE. For very small particle sizes further quantum effects, such as the electron spillout, may become relevant.[26] Even the atomic structure may be important to include.[27] If the system size is small enough, ab initio quantum mechanical calculations can be performed that automatically take into account nonlocal effects, this is known as quantum plasmonics.[28,29] Recently, it has been shown that few-atom systems can support large FEs,[27,30,31] and are surprisingly well-explained by classical plasmonic models,[32,33] which has led to the concept of the quantum plasmonic nanoantenna.[34] Such structures could have applications in

nanolocalized photochemistry where the large field gradients can induce nondipole transitions.

Nonlocality can be modeled via the ingenious method of Luo et al.,[22] where it is mimicked, in local calculations, by the inclusion of a thin (relative to the metal's skin depth) fictitious dielectric boundary layer over the metal. This model has been shown to accurately describe the blue shift of the LSP as well as the smearing of the electric field at boundaries and allows modeling of nonlocality within the computationally simpler local framework.

For nanoparticles smaller than the mean free path, there is an additional surface scattering contribution (also known as Kreibig or Landau damping), which can be simply added to the bulk damping term according to the Matthiessen's rule. The size-dependent term is usually written in the form[35] $\Delta\gamma(R) = A\frac{v_F}{R}$, where A is a parameter on the order of unity, but there exists considerable uncertainty in its value that is a consequence not only of experimental difficulties, but also size-dependent contributions from other sources such as phonon–plasmon coupling,[31,36] structural phase transitions,[37] and adsorbate-induced damping.[38] There have been a number of theoretical[39,40] and experimental[41] works on this topic. Note that the surface scattering model is only a valid picture for symmetrical systems such as the sphere[35] and spherical shell structures[42] and is not easily generalizable to more complicated geometries.

In this work we perform a study of how retardation and nonlocality limits the nanolensing effect and explore the achievable FEs in the classical and quantum limits. We perform an in-depth study of sodium which, due to its simplicity and similarities to the free electron gas, make it ideal for quantum calculations. We consider the effects of nonlocality (i.e., a spatially dispersive longitudinal dielectric function due to quantum effects) and surface-scattering separately and explore the contribution of each in limiting the cascade effect. We find it is the surface scattering that severely limits large FEs in self-similar spherical nanolenses rather than spatial dispersion. We consider the effects of the surface scattering and nonlocality separately but it must be understood that they are two faces of the same coin, namely, a classical representation of a quantum phenomena.

We also consider more realistic plasmonic metals: gold, silver, and aluminum, as well as the polar dielectric silicon carbide (SiC), which supports localized surface phonon polaritons (LSPhPs)[43] and show how a suitable choice of material and the wavelength regime of operation can lead to extreme nanolensing. Further, we compare the nanolens system against dimers of equal volume for silver and SiC. Somewhat surprisingly, we find no benefit of using a silver nanolens compared to the equivalent dimer geometry. In contrast for SiC, we find a substantial benefit of using the nanolens geometry, over a range of geometrical parameters, and find massive FEs approaching 10^4. This leads us to the conclusion that the cascade effect is more suitable for the IR/THz region, where the high quality factor of polar dielectrics and the large size range at which the quasistatic approximation holds leads to nanolens operating close to the idealization originally envisioned by Li et al. and FEs orders of magnitude larger than what can be achieved with metal-based nanolenses.

■ RESULTS AND DISCUSSIONS

Local Calculations for the Sodium Nanolens. We begin by exploring the role of the constituent nanoparticle sizes in a nanolens within the local approximation (in this section we ignore nonlocality) using the boundary element method (BEM).[44−46] Despite the immense interest in the plasmonic cascade mechanism, there has been few detailed studies of the huge parameter space available to modify the near-field response. In Figure 1a, inset, we show the system to be
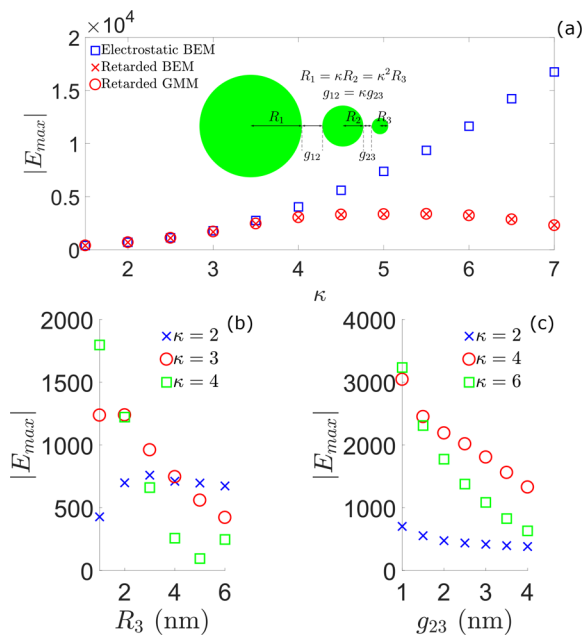

Figure 1. (a) Maximum field enhancement for a sodium nanolens (R_3 = 0.94 nm and g_{23} = 1 nm) for varying κ within the electrostatic approximation (blue) and the full retarded solution (red). As well as the boundary element method solution (crosses), also the generalized Mie theory result is shown for comparison (circles). Shown inset is a schematic of the nanolens studied and the definition of the geometry parameters used in this work. (b) Maximum field enhancement for varying smallest nanoparticle radius (R_3) for different κ. (c) Same but for varying smallest gap size (g_{23}). For all these results, the field is measured 0.3 nm away from the smallest sphere surface in the gap g_{23}.

studied. We use the original geometric progression idea of Li et al.:[2] the smallest particle has a radius R_3, the medium particle has $R_2 = \kappa R_3$ and the largest particle $R_1 = \kappa^2 R_3$. Furthermore, we denote the smallest gap as g_{23} and the larger gap will be $g_{12} = \kappa g_{23}$. The nanolens concept assumes $\kappa \gg 1$, so that the backcoupling of a sphere on its larger neighbor is only a small perturbation.[2] The largest particle acts as an antenna, coupling with the incident light via the dipole mode, and then couples with the higher order modes of the smaller spheres, which can squeeze the light into small volumes.[47] We remark that we enforce this self-similar structure for simplicity but there is no guarantee that it leads to the strongest FEs possible. To explore the FE, we measure the electric field 0.3 nm away from the smallest nanoparticle in the gap between the smallest and medium nanoparticle. Unless otherwise specified, we set the smallest nanoparticle's radius to be 0.94 nm (which corresponds to a closed shell Na_{92} cluster) and the smallest gap to be 1 nm, which it approximately the closest gap size one can achieve before electron tunnelling between the nano-particles can occur (which will limit the maximum FE via short
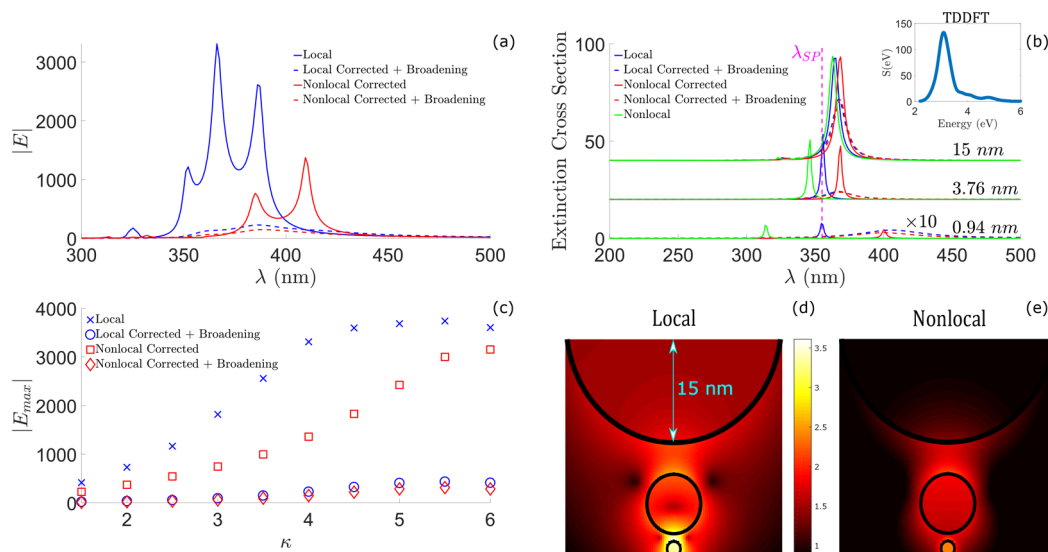
Figure 2. (a) Field enhancement for a nanolens (R_3 = 0.94 nm, g_{23} = 1 nm, and κ = 4) within the four models described in the main text. (b) Extinction cross section for the individual nanospheres for different models; also shown (in green) is the result for the noncorrected nonlocal model. For the smallest nanosphere, the local and nonlocal models with broadening included are multiplied by 10 for clarity. The inset shows the TDDFT result for Na$_{92}$ cluster, where $S(\omega)$ is the dipole strength function. (c) Maximum field enhancement for a range of κ. (d, e) Field profile (logarithmic scale) within the local and nonlocal approximation at the max FE.

circuiting and we do not account for this, it could be included within a classical framework using the quantum corrected model[48]). In Figure 1a, we show a sweep over κ for both electrostatic and full retarded BEM simulations and show the maximum FE over the wavelength range 200 → 500 nm. Unsurprisingly, for low κ ($\lesssim 4$), the electrostatic approximation works well due to the small size of the structure, but already for κ = 4 (which corresponds to the largest particle having a size R_1 = 15 nm), there is a noticeable discrepancy. For larger κ, the FE continues to grow with increasing particles size within the electrostatic approximation, in contrast the retarded calculations show a decrease in EM enhancement with increasing κ as a result of radiative loss and shift of the plasmon resonances for the larger nanospheres. Note that these maximum electric field values may correspond to different spectral positions as the near field resonance will shift in frequency for different geometrical parameters. To confirm our results, we perform a separate calculation using the generalized Mie method (GMM)[49] and find excellent agreement with the BEM. The results clearly show that to achieve strong nanolensing it is desirable to simultaneously have large κ and be within the electrostatic approximation, but this is conflicting requirements and leads to an optimum FE for a given κ.

In Figure 1b, we show the role of the smallest nanoparticle size (R_3) on the maximum FEs achievable for different κ, one can clearly see that the largest FEs are achieved for simultaneously large κ and small R_3. This is a consequence of ignoring nonlocal effects and will not be the case if quantum effects are included. Interestingly, for certain values of R_3, one finds that larger κ is not always advantageous. For instance, for R_3 = 5 nm, the κ = 2 nanolens max FE is 2.7× larger compared to the κ = 4 case; a larger κ is not always best! Similarly, Figure 1c shows the role of the gap size g_{23} and reveals, for larger gap sizes, it may be preferable to use a smaller κ. Together these results reveal the complicated interference effects at play that are captured by the full Maxwell's equations, but not by simple electrostatic models, and illustrate the need for careful

modeling of a nanolens to ensure an optimum choice of parameters is chosen.

Effect of Nonlocality on a Sodium Nanolens. We now include the effects of nonlocality using the local analogue model of Luo et al.[22] within the BEM. Our findings in the last section revealed that it is desirable to choose a small R_3 and large κ, it is interesting to see how this breaks down with quantum effects included. For any practical system, a full numerical quantum calculation is clearly infeasible due to the large size so we make use of a number of approximations to model quantum effects. As the smallest sphere is well within the quantum limit ($R_3 < 1$ nm), we use the spherical jellium model within the local density approximation-TDDFT formalism, which provides a good description for closed shell clusters, to describe the optical response of the individual smallest nanosphere. This provides results accurate to within a few tenths of an electronvolt in comparison to experimental results.[50] We find the TDDFT result does not agree well with the nonlocal model at these sizes for individual nanoparticle optical response, the nonlocal result can be "corrected" following the prescription of Teperik et al.[23] Performing the TDDFT calculation allows an estimation of the electron spill out not possible relying on quasi-quantum nonlocal models and allows modeling of nanolenses down to the quantum limit.

In Figure 2a we show the FE for a sodium nanolens of R_3 = 0.94 nm, g_{23} = 1 nm, and κ = 4 for four different models. The first model is purely local as used in the last section. The second model is local but with surface scattering contribution included in the damping as well as an electron spillout correction to the plasma frequency provided by the TDDFT calculation. Note that for the smallest sphere Na$_{92}$ we use an experimental value of 0.42 eV[50] for the damping rather than the Kreibig formula, which will breakdown at the smallest scale. Sodium is well modeled by a free electron gas and as $\omega_P \gg \gamma$, where ω_P is the plasma frequency and γ is the Drude damping parameter, we may take the plasmon linewidth to be equal to γ. The third model is a nonlocal calculation with both an electron spillout correction and a correction to fix the incorrect value of the

Feibelman parameter for alkali clusters.[23,51] The noncorrected hydrodynamic model predicts the screening charge inside the metal surface leading to a negative Feibelman parameter, this is contradiction to full quantum calculations and experimental results. The plasma frequency can be corrected as

$$\omega_{SP} = \omega_{SP}^{nonloc}\left(1 - \frac{\Delta}{R} - \frac{\delta}{R}\right) \tag{1}$$

where R is the nanosphere radius, Δ is the position of the induced charge relative to the edge, and δ is the spillout length.[23] The local results can be similarly corrected $\omega_{SP} = \omega_{SP}^{loc}\left(1 - \frac{\delta}{R}\right)$, which is done in model 2. Both quantities are on the order of an Å so we will take $\delta \approx \Delta$ and fit according to the TDDFT simulation for a Na_{92} sodium cluster. We find that a value of $\delta = 0.12$ nm gives a good fit to the quantum simulation, this agrees fairly well with the experimental value of 0.145 nm.[52] The fourth model is a nonlocal calculation with the correction and the surface scattering contribution to the damping. Note that the δ parameter is calculated from the single Na_{92} cluster and that value is used for the correction for all the spheres in the nanolens.

By considering these four models, we can explore the contribution from the various small size effects on the FE. In the local model, we find a number of peaks due to a complicated plasmon hybridization between the three particles. Interestingly, compared to the individual nanosphere response, the large FE response is rather broadband; over a range of about 50 nm a large FE of over 1000 is possible. It is also worth remembering that we are only recording the field at one point so there may be large FEs at other points not captured by these results. We find that the nonlocal model with no broadening leads to a redshift (due to electron spillout) and a reduction in the maximum FE to about 40% of the local result, there is also a smoothing out of the number of peaks visible. For both models 2 and 4, there is a serious reduction in the FE by over a factor of 10 due to Landau damping, such a reduction means that the nanolens gives no benefit over ordinary individual nanospheres and dimers that offer FEs on the order of Q and Q^2 respectively,[47] where Q is the quality factor and is on the order of 10 for typical plasmonic metals near the LSP resonance. This leads us to conclude it is the increased damping via surface scattering that severely limits the cascade FE rather than the nonlocal shift of the resonances.

To further understand these results we can analyze the optical response of each individual nanosphere. In Figure 2b, we show the extinction cross section,[53] for each model, of the individual nanoparticles in the $\kappa = 4$ system. Also shown (in green) is the noncorrected nonlocal model for comparison. We can see for the largest particle ($R = 15$ nm) that, somewhat surprisingly, retardation is already important and shifts the resonance to lower energies, at smaller wavelengths we can see a weak higher order mode beginning to form. At all three sizes, we can see that the noncorrected nonlocal model incorrectly predicts a blueshift. The corrected models in contrast show a redshift which is a consequence of the electron spillout, naturally this shift is smaller for larger nanoparticles. For some other metals, such as silver, the nonlocal shift is toward higher energies due to the dynamical screening of d-electrons[51] and the noncorrected nonlocal model will be more accurate, although this should be regarded as a lucky coincidence. It is interesting that for the 15 nm sodium nanoparticle that both retardation and quantum effects have a visible effect, this hints

there is a size regime where fully retarded and quantum calculations are necessary using models such as the recently developed quantum hydrodynamic model.[54] In the inset of Figure 2b, we show the jellium TDDFT result for Na_{92}, where S is the dipole strength function, we use an artificial 0.1 eV broadening. We find close to 3 eV a prominent LSP is present, at lower broadening it is possible to see that in fact the peak is fragmented via interactions with single particle excitations. Also present is a Bennett surface plasmon and the volume plasmon at higher energies,[28] these modes are not included in the local and nonlocal models used. The SPP is red-shifted compared to the classical result due to the soft confining potential.

In Figure 2c, we show the max FE for the four different models over a range of κ. We see that the trends from Figure 2a continue for different values of κ. Interestingly at larger κ, the surface scattering role in decreasing the FE is increased; this is a consequence of the smaller particle not contributing to the cascade effect, while the larger two spheres begin to behave purely classical; in effect, the system behaves as an asymmetric dimer and we can expect FEs on the order of Q^2 rather than Q^3 if surface scattering is not included.[2] We also show a logarithmic plot of the FE for the max FE wavelength at $\kappa = 4$ within the local (model 1) and nonlocal corrected (model 4) in Figure 2d and e, respectively. The local result shows that the largest FE is near the smallest sphere in the gap g_{23}, this agrees with what was found in the original work on the nanolens.[2] In contrast, the FE spatial profile for the nonlocal models shows only a small FE in the gap with the largest fields found solely within the smallest nanoparticle, this illustrates a breakdown of the cascade effect.

It seems from these results that going smaller is not an effective strategy for building plasmonic cascade devices. Recently, similarly drastic reductions (up to 7×) from nonlocality have been shown for the fluorescence enhancement of a dipole near a gold nanoparticle.[55] We emphasize that the inclusion of electron tunnelling, a negligible effect at these gap sizes, would only further limit the FE. It is worth stressing that nonlocality is highly dependent on geometry; for instance, thin metallic nanoshells could offer superior performance for ultrasmall nanolenses. Experimental results have shown that 20 nm thick gold nanoshells show no additional broadening.[56] This has been backed up by theoretical calculations within the random phase approximation, which have shown Landau damping decreases with decreasing nanoshell thickness.[57]

Local Calculations for Gold, Silver, Aluminum, and Silicon Carbide. In the preceding discussions, we have seen the detrimental effects of retardation and nonlocality on the plasmonic cascade effect. To explore different strategies for achieving large FEs, we now consider the effect of the material. We study the effects of changing κ for more typical plasmonic metals: silver, gold, and aluminum. We also look at the polar dielectric SiC which, within the Reststrahlen band that is located in the mid-IR between the longitudinal and transverse optical phonons, behaves as an optical metal and supports LSPhPs.[43] The low loss and high Q (which can be over an order of magnitude larger than for noble metals, this is because the nonradiative loss is determined by phonon−phonon scattering rather than electron−electron scattering in metals) makes polar dielectrics suitable for use in a IR/THz nanolens. Here we study the maximum FE over a range of κ; for simplicity, we use a local model as we now set $R_3 = 5$ nm and $g_{23} = 3$ nm, which are easier for experimental realization and are similar to the geometry used in the original paper by Li et al.[2]

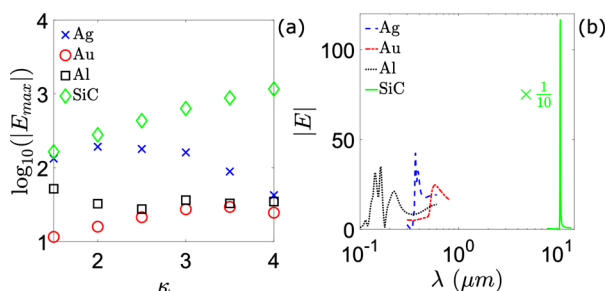In Figure 3 we show the maximum FE 0.3 nm away from the smallest nanosphere. We find that gold, the most commonly

Figure 3. (a) Maximum field enhancement, in log scale, for silver, gold, aluminum, and silicon carbide for different κ. The geometry is R_3 = 5 nm, g_{23} = 3 nm. (b) Field enhancement against wavelength for the $\kappa = 4$ geometry, with the SiC result multiplied by 1/10 to allow visualization.

used plasmonic metal, has the lowest maximum FE: always below 100. This is a consequence of interband transitions close to the plasmon resonance, which limits the quality factor. A more optimum nanolens could be constructed for gold by structuring (for instance into an ellipsoid or rod shape) so that that the LSP is shifted to larger wavelengths. Aluminum exhibits higher FEs and is useful for achieving large FEs in the UV. Silver is a good choice for achieving large FEs due to its large Q for a metal (approximately an order of magnitude larger than gold at the plasmon frequency[43]). Of the four materials, SiC shows the largest FE due to its high Q combined with a lack of retardation loss. In contrast to the monotonically increasing FE with κ for SiC, the metals show a more complicated variation with κ (similar to what is seen for sodium in Figure 1a), which is a hallmark of retardation effects. This is confirmed by comparison with an electrostatic calculation for SiC, which is very similar to the full retarded results. This is a consequence of the low frequency of the SiC LSPhP as compared to the LSP of the metals. The electrostatic approximation holds for a nanosphere, at the resonance, if $|\sqrt{\epsilon}|2\pi R/\lambda_{SPhP} \ll 1$,[53] which for SiC is found to be around a micron; hence, for $\kappa = 4$, where the largest sphere radius is 80 nm, this is very well satisfied still. In comparison, Al, which has a high frequency SPP, very quickly deviates from the electrostatic approximation for very small particle sizes. This suggests that the nanolens concept is more viable for applications in the IR/THz, where the electrostatic approximation holds at larger sizes. Note that the maximum FE is highly sensitive to the material data used, as shown by Pellegrini et al., where the maximum FE was shown to change by a factor of 5, depending on the experimental data used.[58]

The use of SPhPs for the nanolens cascade effect offers an alternative to using LSPs and should lead to larger FEs, although one must work at longer wavelengths in the IR/THz. Fortunately, this is a window of the electromagnetic spectrum that has generated a huge amount of interest, it coincides with vibrational and rotational transitions of molecules.[43] Similar results, using plasmons, may also be obtained in this spectral region for doped semiconductors[59] and graphene.[60] The FE values we have obtained for the SiC nanolens are upper bounds as we have not included any nonlocal or surface scattering corrections; we expect for the systems studied here that such effects will be small and should compare favorably to metals. The flat dispersion of optical phonon in the long wavelength

limit leads to a low group velocity on the order of $\sim 10^4$ m/s for polar crystals; this gives, despite the relatively long scattering time of around $\sim 10^2$ ps, a short mean free path on the order 10 nm. Furthermore, quantum corrections can be expected to be negligible due to an absence of free carriers.

Nanolens versus Dimer. We now comment on the suitability of the cascade effect to achieve large FEs in comparison to the more usual dimer setup. Recently it was suggested by Pellegrini et al.[58] that there are no significant improvements achieved with self-similar nanolenses as compared to plasmonic dimers of equal or less total volume. This was a surprising result but was only tested for a single nanolens geometry; as shown earlier for sodium, the nanolens geometry can vary in a nontrivial fashion for different geometries. Here we explore a range of κ for both silver and SiC. For a fair comparison, we enforce the dimer volume to be equal to the equivalent nanolens for a given κ so that $R_{dimer} = ((R_1^3 + R_2^3 + R_3^3)/2)^{1/3}$, and the gap is the same as the smallest gap (g_{23}) of the nanolens. We measure the field in the middle of the gap for the dimer. There is some arbitrariness when defining a suitable comparison between the dimer and the nanolens; we choose to fix the volume as many physically relevant quantities depend on it, such as the dipole moment and absorption cross section of a sphere. Furthermore, if the volume is not fixed, then the difference in volume between the nanolens and the dimer will change with κ; hence, an analysis based on changing κ would be less meaningful.

In Figure 4a and b is shown the maximum FE over a range of κ for a silver nanolens and the equivalent volume symmetric
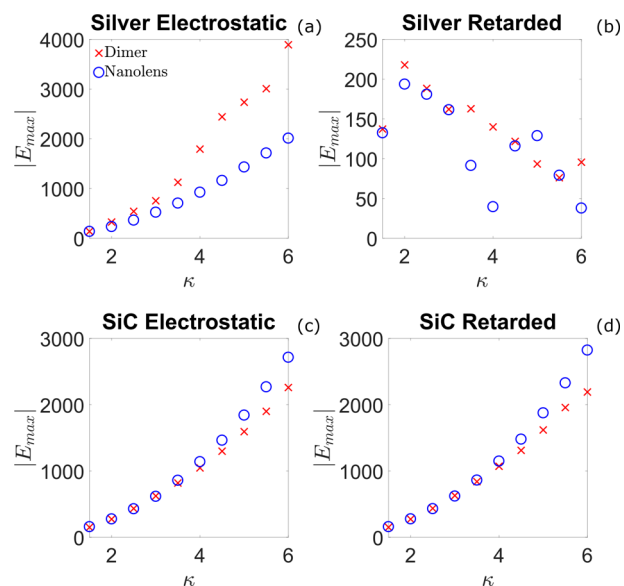

Figure 4. Maximum field enhancement of silver nanolens and dimers for different κ calculated within the electrostatic approximation (a) and full retarded solution (b). The geometry parameters are R_3 = 5 nm and g_{23} = 3 nm. (c, d) Same but for silicon carbide.

dimer for the electrostatic approximation and full retarded solution, respectively. We find for silver that the findings of Pellegrini et al. hold for all geometries considered in the electrostatic approximation and all, except at $\kappa = 5$, for the full retarded calculation. Our work indicates that the nanolens geometry holds no significant advantage over the dimer system in the case of silver for exciting strong FEs. While more work is needed over a larger parameter range and different metals, this

does suggest that the huge amount of work in search for large FEs with nanolenses built of noble metals may be wasted effort when much simpler dimers are preferable. What is most surprising, also noticed by Pellegrini et al.,[58] is that the dimer remains superior within the electrostatic approximation as well (Figure 4a). Thus, it is not retardation effects that limit the nanolensing effect, rather, it is a limitation of the material.

In contrast, for SiC (see Figure 4c,d) we find that the nanolens become increasingly superior to the dimer for larger κ: at $\kappa = 6$ the nanolens geometry leads to a 29% larger FE. The suitability of SiC for nanolensing is a consequence of being well within the electrostatic limit at these sizes, combined with low material loss (large Q). The former being confirmed by the electrostatic results (Figure 4c) being approximately equal to the retarded results (Figure 4d). Note that we expect the nanolens to be further superior to the dimer for larger κ than shown in Figure 4, where we restrict ourselves to $\kappa \leq 6$; the BEM calculations become increasingly difficult to converge as the size ratio between the constituent spheres increases. To confirm this intuition, we have performed an additional calculation (using the multisphere T-matrix code by Mackowski and Mishchenko,[61] which is able to achieve convergence for these challenging geometries) for a $\kappa = 10$ nanolens (see Figure 5a) and find the nanolens geometry has a 82% improvement of
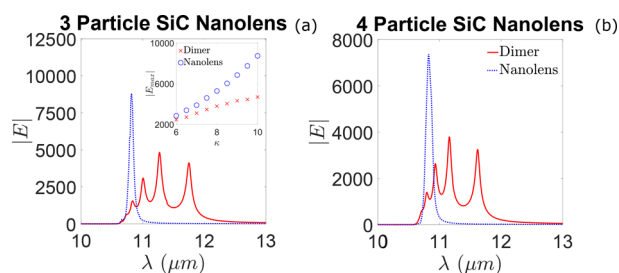

Figure 5. Field enhancement for (a) a 3 particle SiC nanolens of geometry $R_3 = 5$ nm, $g_{23} = 3$ nm, and $\kappa = 10$, and (b) a 4 particle nanolens of geometry $R_4 = 5$ nm, $g_{34} = 3$ nm, and $\kappa = 4$. Both are compared with the equivalent volume dimer.

the maximum FE compared to the equivalent volume dimer. By using SiC structures, we can approach massive FEs of 10^4, which corresponds to an intensity enhancement of 10^8 and the potential for deterministic SERS enhancements of 10^{16}. This demonstrates that polar dielectrics are a suitable material for constructing extreme-cascade nanophotonic devices. The inset of Figure 5a shows the maximum FE for κ from 6 to 10 for both the dimer and the nanolens and shows that the nanolens become increasingly superior for larger κ, continuing the trend from the BEM calculation shown in Figure 4d. The drop off in FE increment with increasing κ for the dimer is presumably due to growing retardation loss; for large enough κ, a similar drop off will be seen for the nanolens. Interestingly, the spectral information in Figure 5a shows that the strongest FE occurs for a narrow single peak and we have found this to be an hallmark of strong nanolensing, this is in contrast to the dimer which has multiple peaks due to mode hybridization. We have confirmed that the response of the system is down to the material resonance rather than a pure geometric resonance by calculating the FE for a silver nanolens in the same wavelength regime as for the SiC nanolens ($10 \rightarrow 13 \, \mu m$), where the silver acts, to a good approximation, as a perfect electrical conductor, and we find only a small FE on the order of 10.

To understand the results shown in Figure 4 further, we model a fictitious Drude model (based on silver) and vary the quality factor. For $\omega \gg \gamma$, this is as simple as changing γ. We then plot the maximum FE of the dimer minus the nanolens for $\kappa = 4$ (see Figure 6). Negative numbers correspond to the
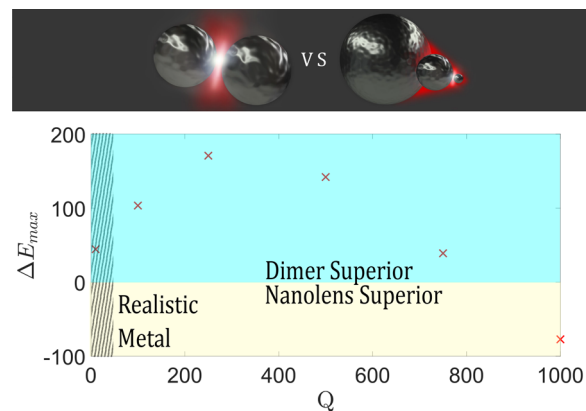

Figure 6. Maximum field enhancement of a dimer minus that of a nanolens for a fictitious Drude metal with variable Q. The geometry parameters are $R_3 = 5$ nm, $g_{23} = 3$ nm, and $\kappa = 4$. Indicated in blue are the regions where the dimer is superior and cream are the region where the nanolens is superior. The hashed region indicated the region of realistic Q values for metals.

nanolens outperforming the dimer. The results show that the nanolens geometry, for these particular parameters, is desirable when the quality factor is very large ($Q \gtrsim 800$), which is far beyond what is achievable in plasmonics in the visible (the Q of silver at the LSP resonance is ~ 30) and is only just within the reach of the best of polar dielectrics at much lower frequencies; SiC has $Q \sim 900$ at the LSPhP resonance.[43] Alternative materials suitable for constructing nanolens could be high index dielectrics which exhibit very large quality factors or hybrid dielectric-metal systems where the loss can be modified over orders of magnitude ($\sim 10^3$) from metal to dielectric-like.[62]

It is worth mentioning that in the original work of Li et al. it was shown that a symmetric nanolens increases the FE by a factor of 2. So far in this work, we have stuck to three self-similar nanospheres, as this corresponds to the most common type of nanolens studied in experiments and will remain in the nanolensing regime for the largest range of κ. Higher FEs can be achieved with a larger number of elements, although at the cost of added complexity to build. Such devices have been experimentally demonstrated[12] and lead to improved SERS intensity[13] compared to the three particle nanolens. In Figure 5b we show the results for a nanolens built of four spheres. The smallest sphere radius (R_4) and gap (g_{34}) are 5 and 3 nm, respectively, and $\kappa = 4$. We find that the nanolens can achieve a maximum FE of almost double the equivalent dimer, again demonstrating the effectiveness of the cascade effect in SiC devices. Higher numbers of nanospheres could be considered and could well lead to even larger improvements. We have also explored four particle silver nanolenses for low κ and observed no significant advantage compared to the equivalent dimer system (result not shown). Interestingly, to observe a consistent advantage for the silver nanolens we had to look at extreme cases such as $R_4 = 1$ nm and $g_{34} = 3$ nm, in the range $1 < \kappa < 2.5$. Of course, this is an unrealistic case as nonlocal effects, which were not included in this calculation, would destroy the nanolensing in reality.

As a final remark, we note that the geometries shown, while demonstrating extreme FE, may be difficult to produce for experimental demonstration due to the large κ and small gaps. These results should be taken as an indication of the ultimate achievable FEs in polar dielectrics (although we emphasize that further geometrical optimization is certainly possible). To demonstrate a more attainable device, we consider a nanolens with both the smallest nanosphere radius and gap to be 10 nm and limit ourselves to $\kappa = 4$, which is inline with what is experimentally achievable. The results are shown in Figure 7,
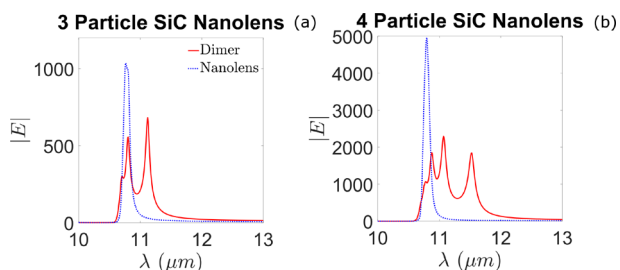

Figure 7. Field enhancement for (a) three and (b) four particle SiC nanolens, with the smallest nanosphere radius and gap equal to 10 nm and $\kappa = 4$. Both are compared with the equivalent volume dimer.

we find for these geometries that the maximum FE is 52% and 116% larger for the 3 and 4 particle nanolens geometry, as compared to the equivalent dimer, respectively. The value of the FE is, of course, lower than the results shown in Figure 5 due to the larger gap. A wider spacing leads to a lower number of higher order plasmon modes being excited and a consequent drop in the field concentration near the smaller nanosphere. The results are clear evidence that experimentally realistic SiC devices can utilize the cascade effect to achieve large FEs, beyond what is achievable with metal based devices.

CONCLUSIONS

We have shown that nonlocal effects hugely limit the possible FE in plasmonics nanolens and have shown that building smaller metallic nanolens to beat retardation is not a viable strategy because of nonlocality. Our top-down approach using quasi-quantum models contrasts with existing studies, based on density functional theory, which have found surprisingly large FEs[27,30,31] and emphasizes the need for a greater understanding of the loss channels relevant to plasmonics at these length scales. A more promising route to achieve large FEs is to use suitable materials or geometries with resonances in the IR/THz where higher quality factors and a much larger span of κ within the electrostatic regime, are possible. In particular, we have illustrated the potential of SiC nanolenses to achieve extreme FEs on the order of 10^4, we can expect even higher FEs for optimized structures. These nanolenses could have applications in molecular sensing in the mid-IR range and could also be suitable for achieving coupling with graphene plasmons and molecular excitations to create tunable hybrid modes.[63] The use of high-index dielectrics for the cascade effect is also promising due to their much superior quality factor compared to metals.

METHODS

For sodium, we use a Drude dielectric function $\epsilon(\omega) = 1 - \frac{\omega_P^2}{\omega^2 + i\omega\gamma}$ with parameters $\omega_P = 6.05$ eV and $\gamma = 0.02684$ eV. The plasma frequency is determined by the

Wigner-Seitz radius 2.08 Å, which is also used to determine the Jellium density. For gold and silver, we use experimental data from Johnson and Christy.[64] For aluminum, Drude parameters of $\omega_P = 15.3$ eV and $\gamma = 0.598$ eV.[65] For SiC we use a Lorentz oscillator model $\epsilon(\omega) = \epsilon_\infty\left(1 + \frac{\omega_L^2 - \omega_T^2}{\omega_T^2 - \omega^2 - i\omega\gamma}\right)$ with the longitudinal and transverse optical phonon frequencies $\omega_T = 0.0988$ eV and $\omega_L = 0.120$ eV, respectively, $\epsilon_\infty = 6.56$ and $\gamma = 0.00059$ eV.[66] Throughout, where possible, we checked local calculations by using both the BEM and GMM method and found excellent agreement.

When using the local analogue model, we set the artificial dielectric thickness to $R/200$ throughout, we have checked the accuracy of the method by comparison to coated Mie theory for a single sphere.[53] For the TDDFT calculations we used the real space code OCTOPUS.[67] To test the validity of our simulation we checked the sum rule $\int s(\omega)d\omega = N$, where N is the number of valence electrons and found it was satisfied to 99.8%.

■ AUTHOR INFORMATION

Corresponding Author
*E-mail: jf1914@ic.ac.uk.

ORCID
Jamie M. Fitzgerald: 0000-0003-3652-0676

Notes
The authors declare no competing financial interest.
Group webpage: www.gianninilab.com.

■ REFERENCES

(1) Maier, S. A. *Plasmonics: Fundamentals and Applications*; Springer Science & Business Media, 2007.
(2) Li, K.; Stockman, M. I.; Bergman, D. J. Self-similar chain of metal nanospheres as an efficient nanolens. *Phys. Rev. Lett.* **2003**, *91*, 227402.
(3) Mayer, K. M.; Hafner, J. H. Localized surface plasmon resonance sensors. *Chem. Rev.* **2011**, *111*, 3828−3857.
(4) Atwater, H. A.; Polman, A. Plasmonics for improved photovoltaic devices. *Nat. Mater.* **2010**, *9*, 205−213.
(5) Kauranen, M.; Zayats, A. V. Nonlinear plasmonics. *Nat. Photonics* **2012**, *6*, 737−748.
(6) Le Ru, E.; Etchegoin, P. *Principles of Surface-Enhanced Raman Spectroscopy: and Related Plasmonic Effects*; Elsevier, 2008.
(7) Bidault, S.; García de Abajo, F. J.; Polman, A. Plasmon-Based Nanolenses Assembled on a Well-Defined DNA Template. *J. Am. Chem. Soc.* **2008**, *130*, 2750−2751.
(8) Kneipp, J.; Li, X.; Sherwood, M.; Panne, U.; Kneipp, H.; Stockman, M. I.; Kneipp, K. Gold nanolenses generated by laser ablation-efficient enhancing structure for surface enhanced Raman scattering analytics and sensing. *Anal. Chem.* **2008**, *80*, 4247−4251.
(9) Ding, B.; Deng, Z.; Yan, H.; Cabrini, S.; Zuckermann, R. N.; Bokor, J. Gold nanoparticle self-similar chain structure organized by DNA origami. *J. Am. Chem. Soc.* **2010**, *132*, 3248−3249.
(10) Kravets, V.; Zoriniants, G.; Burrows, C. P.; Schedin, F.; Casiraghi, C.; Klar, P.; Geim, A.; Barnes, W. L.; Grigorenko, A. Cascaded optical field enhancement in composite plasmonic nanostructures. *Phys. Rev. Lett.* **2010**, *105*, 246806.

(11) Höppener, C.; Lapin, Z. J.; Bharadwaj, P.; Novotny, L. Self-similar gold-nanoparticle antennas for a cascaded enhancement of the optical field. *Phys. Rev. Lett.* **2012**, *109*, 017402.

(12) Coluccio, M. L.; Gentile, F.; Das, G.; Nicastri, A.; Perri, A. M.; Candeloro, P.; Perozziello, G.; Zaccaria, R. P.; Gongora, J. S. T.; Alrasheed, S.; Fratalocchi, A.; Limongi, T.; Cuda, G.; Di Fabrizio, E. Detection of single amino acid mutation in human breast cancer by disordered plasmonic self-similar chain. *Science advances* **2015**, *1*, e1500487.

(13) Das, G.; Alrasheed, S.; Coluccio, M. L.; Gentile, F.; Nicastri, A.; Candeloro, P.; Cuda, G.; Perozziello, G.; Di Fabrizio, E. Few molecule SERS detection using nanolens based plasmonic nanostructure: application to point mutation detection. *RSC Adv.* **2016**, *6*, 107916−107923.

(14) Heck, C.; Prinz, J.; Dathe, A.; Merk, V.; Stranik, O.; Fritzsche, W.; Kneipp, J.; Bald, I. Gold nanolenses self-assembled by DNA origami. *ACS Photonics* **2017**, *4*, 1123.

(15) Lloyd, J. A.; Ng, S. H.; Liu, A. C.; Zhu, Y.; Chao, W.; Coenen, T.; Etheridge, J.; Gómez, D. E.; Bach, U. Plasmonic Nanolenses: Electrostatic Self-Assembly of Hierarchical Nanoparticle Trimers and Their Response to Optical and Electron Beam Stimuli. *ACS Nano* **2017**, *11*, 1604−1612.

(16) Heck, C.; Kanehira, Y.; Kneipp, J.; Bald, I. Single proteins placed within the SERS hot spots of self-assembled silver nanolenses. *Angew. Chem.* **2018**, na.

(17) Li, Z.; Yang, Z.; Xu, H. Comment on "Self-similar chain of metal nanospheres as an efficient nanolens. *Phys. Rev. Lett.* **2006**, *97*, 079701.

(18) Dai, J.; Čajko, F.; Tsukerman, I.; Stockman, M. I. Electrodynamic effects in plasmonic nanolenses. *Phys. Rev. B: Condens. Matter Mater. Phys.* **2008**, *77*, 115419.

(19) McMahon, J. M.; Gray, S. K.; Schatz, G. C. Nonlocal optical response of metal nanostructures with arbitrary shape. *Phys. Rev. Lett.* **2009**, *103*, 097403.

(20) David, C.; García de Abajo, F. J. Spatial nonlocality in the optical response of metal nanoparticles. *J. Phys. Chem. C* **2011**, *115*, 19470−19475.

(21) Toscano, G.; Raza, S.; Jauho, A.-P.; Mortensen, N. A.; Wubs, M. Modified field enhancement and extinction by plasmonic nanowire dimers due to nonlocal response. *Opt. Express* **2012**, *20*, 4176−4188.

(22) Luo, Y.; Fernandez-Dominguez, A.; Wiener, A.; Maier, S. A.; Pendry, J. Surface plasmons and nonlocality: a simple model. *Phys. Rev. Lett.* **2013**, *111*, 093901.

(23) Teperik, T. V.; Nordlander, P.; Aizpurua, J.; Borisov, A. G. Robust subnanometric plasmon ruler by rescaling of the nonlocal optical response. *Phys. Rev. Lett.* **2013**, *110*, 263901.

(24) Mortensen, N. A.; Raza, S.; Wubs, M.; Søndergaard, T.; Bozhevolnyi, S. I. A generalized non-local optical response theory for plasmonic nanostructures. *Nat. Commun.* **2014**, *5*, na.

(25) Schnitzer, O.; Giannini, V.; Maier, S. A.; Craster, R. V. Surface plasmon resonances of arbitrarily shaped nanometallic structures in the small-screening-length limit. *Proc. R. Soc. London, Ser. A* **2016**, *472*, 20160258.

(26) Toscano, G.; Straubel, J.; Kwiatkowski, A.; Rockstuhl, C.; Evers, F.; Xu, H.; Mortensen, N. A.; Wubs, M. Resonance shifts and spill-out effects in self-consistent hydrodynamic nanoplasmonics. *Nat. Commun.* **2015**, *6*, na.

(27) Zhang, P.; Feist, J.; Rubio, A.; García-González, P.; García-Vidal, F. Ab initio nanoplasmonics: The impact of atomic structure. *Phys. Rev. B: Condens. Matter Mater. Phys.* **2014**, *90*, 161407.

(28) Varas, A.; García-González, P.; Feist, J.; García-Vidal, F.; Rubio, A. Quantum plasmonics: from jellium models to ab initio calculations. *Nanophotonics* **2016**, *5*, 409−426.

(29) Fitzgerald, J. M.; Narang, P.; Craster, R. V.; Maier, S. A.; Giannini, V. Quantum Plasmonics. *Proc. IEEE* **2016**, *104*, 2307−2322.

(30) Bursi, L.; Calzolari, A.; Corni, S.; Molinari, E. Light-induced field enhancement in nanoscale systems from first-principles: the case of polyacenes. *ACS Photonics* **2014**, *1*, 1049−1058.

(31) Fitzgerald, J. M.; Azadi, S.; Giannini, V. Quantum plasmonic nanoantennas. *Phys. Rev. B: Condens. Matter Mater. Phys.* **2017**, *95*, 235414.

(32) Sinha-Roy, R.; Garcia-Gonzalez, P.; Weissker, H.-C.; Rabilloud, F.; Fernandez-Dominguez, A. I. Classical and ab Initio Plasmonics Meet at Sub-nanometric Noble Metal Rods. *ACS Photonics* **2017**, *4*, 1484−1493.

(33) Urbieta, M.; Barbry, M.; Zhang, Y.; Koval, P.; Sánchez-Portal, D.; Zabala, N.; Aizpurua, J. Atomic-Scale Lightning Rod Effect in Plasmonic Picocavities: a Classical View to a Quantum Effect. *ACS Nano* **2018**, *12*, 585.

(34) Fitzgerald, J. M.; Giannini, V. Perspective on molecular quantum plasmonic nanoantennas. *J. Opt.* **2017**, *19*, 060401.

(35) Kreibig, U.; Vollmer, M. *Optical Properties of Metal Clusters*; Springer Science & Business Media, 2013; Vol. 25.

(36) Donati, G.; Lingerfelt, D. B.; Aikens, C. M.; Li, X. Molecular Vibration Induced Plasmon Decay. *J. Phys. Chem. C* **2017**, *121*, 15368.

(37) Kreibig, U. The transition cluster-solid state in small gold particles. *Solid State Commun.* **1978**, *28*, 767−769.

(38) Pinchuk, A.; Kreibig, U. Interface decay channel of particle surface plasmon resonance. *New J. Phys.* **2003**, *5*, 151.

(39) Molina, R. A.; Weinmann, D.; Jalabert, R. A. Oscillatory size dependence of the surface plasmon linewidth in metallic nanoparticles. *Phys. Rev. B: Condens. Matter Mater. Phys.* **2002**, *65*, 155427.

(40) Lermé, J.; Baida, H.; Bonnet, C.; Broyer, M.; Cottancin, E.; Crut, A.; Maioli, P.; Del Fatti, N.; Vallée, F.; Pellarin, M. Size dependence of the surface plasmon resonance damping in metal nanospheres. *J. Phys. Chem. Lett.* **2010**, *1*, 2922−2928.

(41) Quinten, M. Optical constants of gold and silver clusters in the spectral range between 1.5 and 4.5 eV. *Z. Phys. B: Condens. Matter* **1996**, *101*, 211−217.

(42) Moroz, A. Electron mean free path in a spherical shell geometry. *J. Phys. Chem. C* **2008**, *112*, 10641−10652.

(43) Caldwell, J. D.; Lindsay, L.; Giannini, V.; Vurgaftman, I.; Reinecke, T. L.; Maier, S. A.; Glembocki, O. J. Low-loss, infrared and terahertz nanophotonics using surface phonon polaritons. *Nanophotonics* **2015**, *4*, 44−68.

(44) De Abajo, F. G.; Howie, A. Retarded field calculation of electron energy loss in inhomogeneous dielectrics. *Phys. Rev. B: Condens. Matter Mater. Phys.* **2002**, *65*, 115418.

(45) Hohenester, U.; Trügler, A. MNPBEM-A Matlab toolbox for the simulation of plasmonic nanoparticles. *Comput. Phys. Commun.* **2012**, *183*, 370−381.

(46) Waxenegger, J.; Trügler, A.; Hohenester, U. Plasmonics simulations with the MNPBEM toolbox: Consideration of substrates and layer structures. *Comput. Phys. Commun.* **2015**, *193*, 138−150.

(47) Sun, G.; Khurgin, J. B.; Bratkovsky, A. Coupled-mode theory of field enhancement in complex metal nanostructures. *Phys. Rev. B: Condens. Matter Mater. Phys.* **2011**, *84*, 045415.

(48) Esteban, R.; Borisov, A. G.; Nordlander, P.; Aizpurua, J. Bridging quantum and classical plasmonics with a quantum-corrected model. *Nat. Commun.* **2012**, *3*, 825.

(49) Pellegrini, G.; Mattei, G.; Bello, V.; Mazzoldi, P. Interacting metal nanoparticles: Optical properties from nanoparticle dimers to core-satellite systems. *Mater. Sci. Eng., C* **2007**, *27*, 1347−1350.

(50) Xia, C.; Yin, C.; Kresin, V. V. Photoabsorption by volume plasmons in metal nanoclusters. *Phys. Rev. Lett.* **2009**, *102*, 156802.

(51) Monreal, R. C.; Antosiewicz, T. J.; Apell, S. P. Competition between surface screening and size quantization for surface plasmons in nanoparticles. *New J. Phys.* **2013**, *15*, 083044.

(52) Reiners, T.; Ellert, C.; Schmidt, M.; Haberland, H. Size dependence of the optical response of spherical sodium clusters. *Phys. Rev. Lett.* **1995**, *74*, 1558.

(53) Bohren, C. F.; Huffman, D. R. *Absorption and scattering of light by small particles*; John Wiley & Sons, 2008.

(54) Yan, W. Hydrodynamic theory for quantum plasmonics: Linear-response dynamics of the inhomogeneous electron gas. *Phys. Rev. B: Condens. Matter Mater. Phys.* **2015**, *91*, 115416.

(55) Jurga, R.; D'Agostino, S.; della Sala, F.; Ciraci, C. Plasmonic Nonlocal Response Effects on Dipole Decay Dynamics in the Weak and Strong-Coupling Regimes. *J. Phys. Chem. C* **2017**, *121*, 22361.

(56) Nehl, C. L.; Grady, N. K.; Goodrich, G. P.; Tam, F.; Halas, N. J.; Hafner, J. H. Scattering spectra of single gold nanoshells. *Nano Lett.* **2004**, *4*, 2355−2359.

(57) Kirakosyan, A. S.; Stockman, M. I.; Shahbazyan, T. V. Surface plasmon lifetime in metal nanoshells. *Phys. Rev. B: Condens. Matter Mater. Phys.* **2016**, *94*, 155429.

(58) Pellegrini, G.; Celebrano, M.; Finazzi, M.; Biagioni, P. Local field enhancement: comparing self-similar and dimer nanoantennas. *J. Phys. Chem. C* **2016**, *120*, 26021−26024.

(59) Luther, J. M.; Jain, P. K.; Ewers, T.; Alivisatos, A. P. Localized surface plasmon resonances arising from free carriers in doped quantum dots. *Nat. Mater.* **2011**, *10*, 361.

(60) Koppens, F. H.; Chang, D. E.; García de Abajo, F. J. Graphene plasmonics: a platform for strong light-matter interactions. *Nano Lett.* **2011**, *11*, 3370−3377.

(61) Mackowski, D.; Mishchenko, M. A multiple sphere T-matrix Fortran code for use on parallel computer clusters. *J. Quant. Spectrosc. Radiat. Transfer* **2011**, *112*, 2182−2192.

(62) Yang, Y.; Miller, O. D.; Christensen, T.; Joannopoulos, J. D.; Soljacic, M. Low-loss Plasmonic Dielectric Nanoresonators. *Nano Lett.* **2017**, *17*, 3238−3245.

(63) Li, K.; Fitzgerald, J. M.; Xiao, X.; Caldwell, J. D.; Zhang, C.; Maier, S. A.; Li, X.; Giannini, V. Graphene Plasmon Cavities Made with Silicon Carbide. *ACS Omega* **2017**, *2*, 3640−3646.

(64) Johnson, P. B.; Christy, R.-W. Optical constants of the noble metals. *Phys. Rev. B* **1972**, *6*, 4370.

(65) Blaber, M. G.; Arnold, M. D.; Ford, M. J. Search for the ideal plasmonic nanoshell: the effects of surface scattering and alternatives to gold and silver. *J. Phys. Chem. C* **2009**, *113*, 3041−3045.

(66) Francescato, Y. New frequencies and geometries for plasmonics and metamaterials. *PhD. thesis*, Imperial College London, 2014.

(67) Andrade, X.; et al. Real-space grids and the Octopus code as tools for the development of new simulation approaches for electronic systems. *Phys. Chem. Chem. Phys.* **2015**, *17*, 31371−31396.